Small molecules targeting severe acute respiratory syndrome human coronavirus

Chung-Yi Wu*, Jia-Tsrong Jan†‡, Shiou-Hwa Ma†, Chih-Jung Kuo*, Hsueh-Fen Juan§, Yih-Shyun E. Cheng*, Hsien-Hua Hsu*, Hsuan-Cheng Huang*, Douglass Wu¶, Ashraf Brik¶, Fu-Sen Liang¶, Rai-Shung Liu‖, Jim-Min Fang*,, Shui-Tein Chen*, Po-Huang Liang*, and Chi-Huey Wong*¶††**

*Genomics Research Center and Institute of Biological Chemistry, Academia Sinica, Taipei 115, Taiwan; †Institute of Preventive Medicine, National Defense Medical Center, National Defense University, Taipei 114, Taiwan; §Department of Chemical Engineering, National Taipei University of Technology, Taipei 106, Taiwan; **Department of Chemistry, National Taiwan University, Taipei 106, Taiwan; ¶Department of Chemistry and The Skaggs Institute for Chemical Biology, The Scripps Research Institute, La Jolla, CA 92037; and ‖Department of Chemistry, National Tsing Hua University, Hsinchu 300, Taiwan

Contributed by Chi-Huey Wong, May 26, 2004

Severe acute respiratory syndrome (SARS) is an infectious disease caused by a novel human coronavirus. Currently, no effective antiviral agents exist against this type of virus. A cell-based assay, with SARS virus and Vero E6 cells, was developed to screen existing drugs, natural products, and synthetic compounds to identify effective anti-SARS agents. Of >10,000 agents tested, ≈50 compounds were found active at 10 μM; among these compounds, two are existing drugs (Reserpine 13 and Aescin 5) and several are in clinical development. These 50 active compounds were tested again, and compounds 2–6, 10, and 13 showed active at 3 μM. The 50% inhibitory concentrations for the inhibition of viral replication (EC_{50}) and host growth (CC_{50}) were then measured and the selectivity index ($SI = CC_{50}/EC_{50}$) was determined. The EC_{50}, based on ELISA, and SI for Reserpine, Aescim, and Valinomycin are 3.4 μM (SI = 7.3), 6.0 μM (SI = 2.5), and 0.85 μM (SI = 80), respectively. Additional studies were carried out to further understand the mode of action of some active compounds, including ELISA, Western blot analysis, immunofluorescence and flow cytometry assays, and inhibition against the 3CL protease and viral entry. Of particular interest are the two anti-HIV agents, one as an entry blocker and the other as a 3CL protease inhibitor (K_i = 0.6 μM).

Severe acute respiratory syndrome (SARS) is an acute respiratory illness caused by infection with a novel human coronavirus (SARS-CoV) (1, 2). The first SARS case was found in Guangdong, South China, in November 2002, and since then the disease has spread to >25 countries. By July 31, 2003, 8,098 SARS cases and 774 SARS-related deaths were reported around the world. Studies on the molecular evolution of SARS-CoV suggested that the virus emerged from non-human sources (3).

At present, the combination of Ribavirin and corticosteroids is the most frequently administered antiviral agent for SARS (4–12). However, Ribavirin at nontoxic concentrations has little *in vitro* activity against SARS-CoV (13) and has many side effects (9). An improved clinical outcome was reported among SARS patients receiving early administration with the HIV drug Kaletra plus Ribavirin and corticosteroids (14). Glycyrrhizin (13) and human interferons (15, 16) were also reported to be effective against SARS. However, no clear evidence was demonstrated to support these clinical observations. Therefore, the search for more effective and potent antivirals for the SARS virus is of current interest. Recent identification of the viral genome (17–19), the viral receptor (20), the viral main protease (the chymotrypsin-like protease, also called 3CL protease) and its structure (21, 22), and activity studies (23, 24) have provided a better understanding of this devastating disease and should facilitate the development of effective therapeutic agents. This report describes a cell-based assay using SARS-CoV and Vero E6 cells (18) to screen a collection of nearly 10,000 compounds and natural products to identify antiviral agents for SARS. It also describes further studies of some promising lead compounds revealed from the screen.

Materials and Methods

The agents tested in this study include ≈200 drugs approved by the Food and Drug Administration, >8,000 synthetic compounds, ≈1,000 traditional Chinese herbs, and ≈500 protease inhibitors.

Compounds were dissolved in DMSO to 10 mM and transferred to 96-well microtiter plates to assay for antiviral activity based on the prevention of the SARS-virus-mediated cytopathic effect. Additional confirmative studies were done by cytotoxicity, immunofluorenscence ELISA, Western blot analysis, flow cytometry on viral protein expression with SARS-CoV-spike protein-specific monoclonal antibodies, and protease inhibition.

Primary Screening for Anti-SARS-CoV Compounds. Vero E6 cells (2×10^4 per well) were cultured in a 96-well plate in DMEM supplemented with 10% FBS. The culture medium was removed after a 1-day incubation when the cells reached 80–90% confluence. A solution of 100 μl of DMEM, with 2% FBS containing the compound to be tested, was placed in three wells. Cells were incubated in a CO_2 incubator at 37°C for 2 h and inoculated with SARS-CoV (H.K. strain) at a dose of 100 $TCID_{50}$ per well; the cytopathic morphology of the cells was examined by using an inverted microscope 72 h after infection.

Cytotoxicity Study of Compounds with Vero E6 Cells. Vero E6 cells were grown in a humidified 5% CO_2 incubator at 37°C in DMEM supplemented with L-glutamine, nonessential amino acids, and 10% FBS, and they were seeded at 7×10^4 cells per ml onto a 96-well plate and left overnight.

3-(4,5-Dimethylthiazole-2-yl)-5-(3-carboxy-methoxyphenyl)-2-(4-sulfophenyl)-2H-tetrazolium, inner salt (MTS) assay was performed by using CellTiter 96 Aqueous Non-radioactive Cell Proliferation Assay Kits (Promega) to determine the population of living cells. In brief, after the incubations with compounds at varied concentrations for 2 days, the culture medium was replaced with 100 μl MTS/phenazine methosulfate in DMEM, incubated at 37°C for 2 h, and measured with a plate reader at 490 nm. Data are expressed as percentage of control cells (as 100%) cultured in the absence of any compounds.

ELISA. At the conclusion of the incubation, the SARS-virus-infected Vero E6 cells were rinsed with PBS and fixed in a

Abbreviations: SARS, severe acute respiratory syndrome; CoV, coronavirus; IFA, immunofluorescence assay; SI, selectivity index; MTS, 3-(4,5-dimethylthiazole-2-yl)-5-(3-carboxymethoxyphenyl)-2-(4-sulfophenyl)-2H-tetrazolium, inner salt.

‡To whom correspondence may be sent at the † address. E-mail: tsrong33@pchome.com.tw1.

††To whom correspondence may be addressed at: The Scripps Research Institute, 10550 North Torrey Pines Road, La Jolla, CA 92037, and Genomics Research Center, Academia Sinica, Taipei 115, Taiwan. E-mail: wong@scripps.edu or chwong@gate.sinica.edu.tw.

www.pnas.org/cgi/doi/10.1073/pnas.0403596101

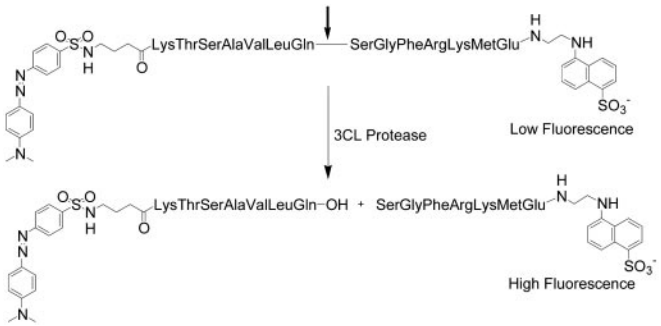

Fig. 1. The fluorogenic substrate used for SARS-CoV 3CL protease inhibition assay. Enhanced fluorescence caused by cleavage of the fluorogenic substrate peptide was monitored at 538 nm with excitation at 355 nm.

solution containing ice methanol/acetone (1:1) solution for 5 min at room temperature and rinsed three times with PBS. Cells were blocked with 3% skimmed milk in PBS for 2 h at room temperature and then incubated for 1 h at 37°C with 1:2,000 diluted monoclonal antibody (ascetic fluid) to the spike protein of SARS-CoV. All samples were washed with three changes of PBS-T buffer and twice with fresh changes of PBS buffer at room temperature, followed by a 30-min incubation with horseradish peroxidase-labeled goat anti-mouse IgG for 30 min at room temperature. Plates were rinsed with PBS containing 0.05% Tween 20 between incubations. A substrate solution containing *O*-phenylenediamine dihydrochloride, citrate buffer (pH 5.0), and hydrogen peroxide was added to each well. Plates were covered and gently shaken at room temperature for 10 min. The reaction was stopped by the addition of 3 N sulfuric acid, and plates were read immediately at 492 nm. The EC_{50} value for each agent was extrapolated from the linear regression plot of agent concentration versus OD_{492}.

Immunofluoresence Assay (IFA). Infected or control cells were rinsed with PBS and resuspended to a final concentration of 1×10^6 cells per ml. Slides were prepared for IFA by spotting wells with 2×10^4 cells for each agent concentration and controls, then dried, fixed in ice methanol/acetone (1:1) solution for 3 min, then rinsed, and stored at −20°C before staining for IFA. Daudi cells were rehydrated then blocked with 3% skimmed milk in PBS for 30 min at room temperature. Vero E6 cells were rehydrated, blocked, and permeabilized in PBS containing 0.1% saponin and 1% FBS. Cells were then incubated in a hydration chamber at 37°C for 1 h with 20 μl of primary antibody in a blocking solution. After a rinse with PBS, cells were incubated at 37°C for 1 h FITC-conjugated goat anti-mouse IgG + IgM secondary antibody (Jackson ImmunoResearch), and rinsed with PBS before staining with 0.1% Evans blue dye (Fisher) in PBS for 5 min. Slides were rinsed to remove any excess contrast dye and cover slides were mounted by using a solution of 50% glycerol in PBS. Cells were viewed at a magnification of ×400 with a Nikon fluorescence microscope. For each agent concentration, 500 cells were counted and the percentage of antigen-positive cells was calculated. The agent concentration required to inhibit virus replication by 50% (EC_{50}) was determined.

Western Blot Analysis of Anti-SARS Agents. SARS-CoV-infected Vero E6 cells were treated with compounds at varied concentrations for 24 or 48 h then lysed in a lysis buffer for 3 min. The cell debris was spun down and all cell lysates were harvested for electrophoresis and Western blotting assay with SDS/PAGE and a Hybond-C Extra membrane (Amersham Pharmacia). The resulting membrane was blocked in 3% skimmed milk in PBS for 30 min at room temperature and then treated with 1:1,000 diluted anti-spike protein monoclonal antibody (Chemicon MAb 1501) for 1 h at room temperature. The membrane was rinsed by using two changes of PBS-T buffer and then washed once for 15 min and twice for 5 min each with fresh PBS buffer at room temperature, followed by treatment with horseradish peroxidase-labeled goat anti-mouse IgG for 30 min and 1:2,000 dilution for 1 h. The membrane was washed as above and the mixed enhanced chemiluminescence detection reagent was added to the protein side of the membrane. The blot was placed with the protein side up, in the film cassette, to visualize the level of protein expression.

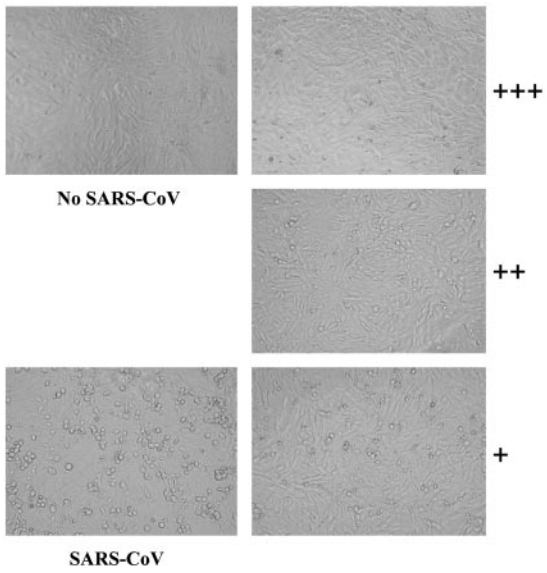

Fig. 2. The test for cytopathogenic effects. +++ indicates that the protective effect is obvious, and ++ and + indicate moderate and weak, respectively.

Flow Cytometry Analysis of Anti-SARS Activities. Vero E6 cells were rinsed and blocked with 5% FBS and 4% goat serum in PBS. SARS-CoV-infected cells were trypsinized with 0.05% trypsin-EDTA medium, and ≈1–5 × 10^5 cells were distributed to each well of a round-bottom ELISA plate. The suspension was centrifuged and the cells were rinsed with PBS and thoroughly resuspended; 100 μl of Cytofix/Cytoperm solution was added to each well, then fixed and permeabilized in 2 μl of methanol for 20 min at 4°C. These cells were blocked in PBS containing 5% FBS, 4% serum, and 0.5% DMSO for 30 min at 37°C. Samples were incubated with 20 μl of primary antibody diluted in blocking solution for 1 h at 37°C, then rinsed twice with blocking solution, and pelleted by centrifugation at 1,000 × *g* for 5 min. After the second rinse, 0.5 μl of 3 μg/ml FITC-conjugated goat anti-mouse IgG + IgM was added followed by incubation for 1 h at 37°C. Cells were rinsed twice with PBS and pelleted by centrifugation before being resuspended.

Flow cytometry data were acquired by using a Becton Dickinson FACSCalibur instrument, and data were analyzed by using the WIN-MDI 2.7 data analysis program (The Scripps Research Institute). The resulting dot plots were gated to remove nonspecific and background staining from further consideration, and the M1 bar was set so that <1% of the cells in the negative control were included in the determination of percent positive cells. The EC_{50} value for each agent was extrapolated from the plot of agent concentration versus percentage of antigen-positive cells as described above.

SARS-CoV 3CL-Protease Inhibition Assay. As described (25), the gene encoding the SARS-CoV main protease was cloned from

the viral whole genome by using PCR with the forward primer 5′-GGTATTGAGGGTCGCA-GTGGTTTTAGG-3′ and reverse primer 5′-AGAGGAGAGTTAGAGCCTTATTGG-AAGGTAACACC-3′ into the pET32Xa/LIC vector. The FXa cleavage site (IEGR) and the complementary sequences to the sticky ends of the linear vector pET-32Xa/LIC were included in these primers. The recombinant protease plasmid was then used to transform *Escherichia coli* JM109 competent cells that were streaked on a LB agar plate containing 100 μg/ml ampicillin. The correct construct was subsequently transformed into *E. coli* BL21 for expression of the His-tagged protein, which was then digested with FXa protease to remove the tag. The purified protein was confirmed by N-terminal sequencing and MS. The enzyme concentration used in all experiments was determined from the absorbance at 280 nm.

All kinetic measurements were performed in 20 mM bis(2-hydroxyethyl)amino]tris(hydroxymethyl)methane (pH 7.0) at 25°C. Enhanced fluorescence due to cleavage of the fluorogenic substrate peptide (Dabcyl-KTSAVLQ-SGFRKME-Edans) was monitored at 538 nm with excitation at 355 nm (Fig. 1) by using a fluorescence plate reader (Fluoroskan Ascent, ThermoLabsystems, Helsinki, Finland).

The initial velocities of the inhibited reactions of 50 nM SARS main protease and 6 μM fluorogenic substrate were plotted against the different inhibitor concentrations to obtain the IC_{50} by using the following equation.

$$A[I] = A[0] \times \{1 - [[I]/([I] + IC_{50})]\} \quad [1]$$

$A[I]$ is the enzyme activity with inhibitor concentration $[I]$; $A[0]$ is the enzyme activity without inhibitor.

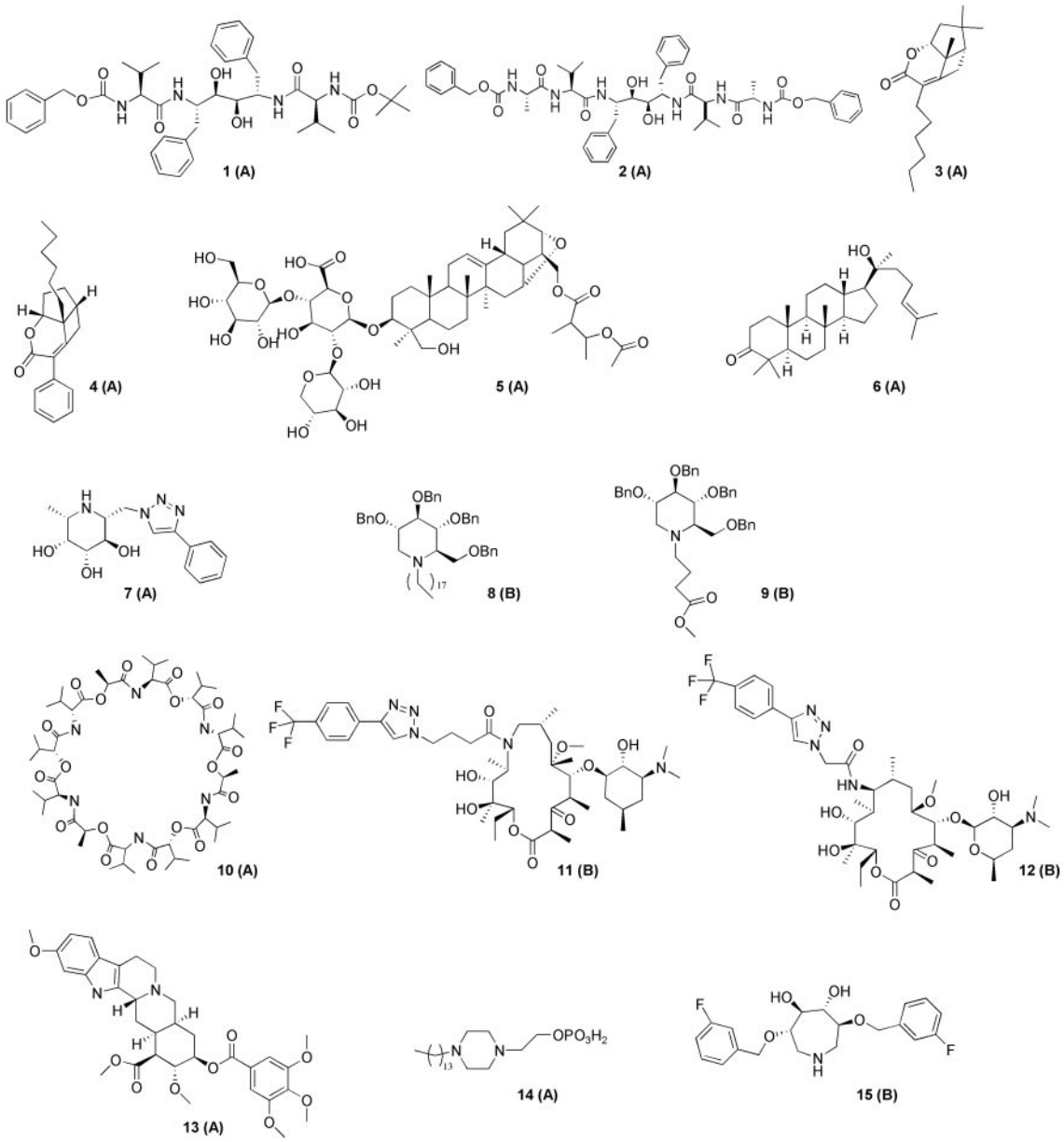

Fig. 3. Representative compounds showed protective effect at 10 μM. Parentheses indicate the result of cytotoxicity. (A) indicates the compounds that are noninhibitory to Vero E6 at concentrations greater than four times the anti-SARS concentrations. (B) indicates compounds that are noninhibitory at the anti-SARS concentrations. However, growth retardation, to ≈80% of the control level, was observed when Vero E6 cells were treated with these compounds at two times the anti-SARS concentrations.

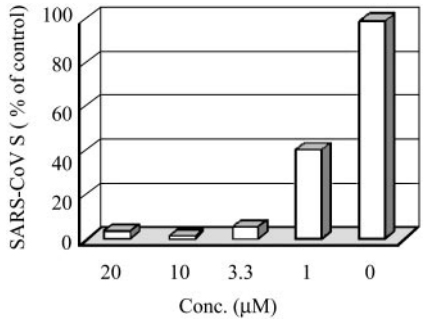

Fig. 4. ELISA of SARS-CoV spike protein in response to compound **10** treatment. % of control = (OD of SARS-CoV Inf. − OD of Mock.Inf. [Conc. *x*])/(OD of SARS-CoV. Inf. − OD of Mock-Inf. [Conc. 0]). EC_{50} = 0.85 μM; S.I. = 80. Inf., infection.

K_i measurements were performed at two fixed inhibitor concentrations and various substrate concentrations ranging from 8 to 80 μM in a reaction mixture containing 50 nM SARS protease. Lineweaver–Burk plots of kinetic data were fitted with the computer program KINETASYST II (IntelliKinetics, State College, PA) by nonlinear regression to obtain the K_i value of a competitive inhibitor from the following equation.

$$1/V = K_m/V_m[S]\cdot(1 + [I]/K_i) + 1/V_m \quad [2]$$

Computer Modeling of SARS-CoV 3CL Protease Inhibition. Docking calculations were completed by using AUTODOCK V. 3.0 (26) with the Genetic Algorithm. Protein coordinates were taken from the crystallographic structure of SARS-Co-V M^{Pro} (PDB ID code 1UJ1) (21).

Results and Discussion

Primary Cell-Based Screening. We initially used the observed cytopathogenic effect on Vero E6 cells to assess the antiviral activity of compounds at a concentration of 10 μM (Fig. 2). Of >10,000 compounds tested, ≈50 showed protective effects. Representative structures of active compounds are shown in Fig. 3.

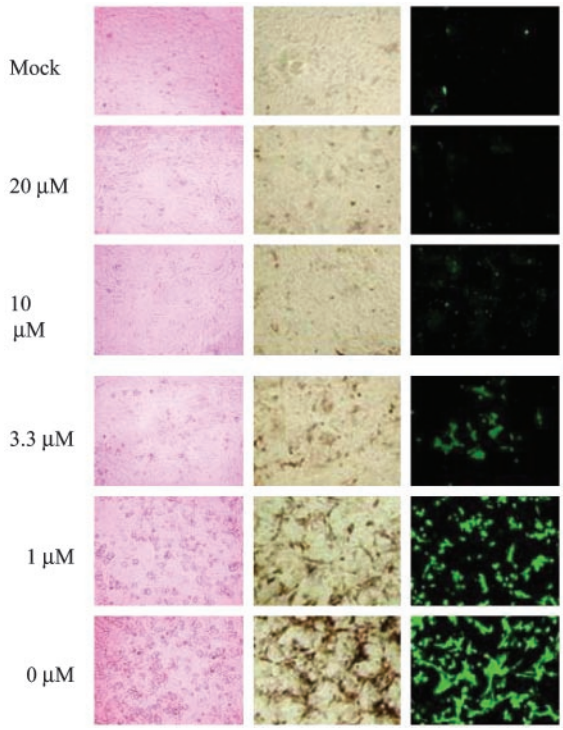

Fig. 5. Compound **10**-inhibited cytopathic effect induced by SARS-CoV and the viral protein expression shown by IFA.

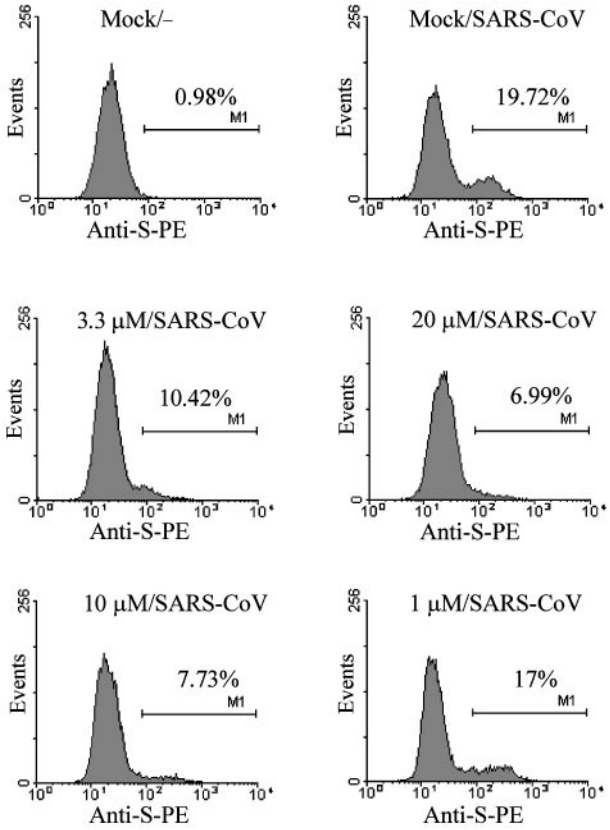

Fig. 6. Flow cytometry analysis of the inhibitory effect of compound **10** on SARS-CoV. S, spike protein; PE, phycoerythrin (a red fluorescent dye). The PE value represents the level of viral spike protein expression.

Cytotoxicity Study of Anti-SARS Compounds Using Vero E6 Cells. Because any compound that is inhibitory to cell growth may exhibit an apparent antiviral activity, it is thus important to evaluate the inhibitory effects of all anti-SARS compounds on the growth of host cells. The cytotoxicity study on Vero E6 cells was undertaken by comparison of the live cells after a 2-day incubation with anti-SARS compounds at varied concentrations. The number of live cells was determined by using the MTS assay (27).

Among the compounds in Fig. 3, those that are not inhibitory to the growth of Vero E6 cells at concentrations greater than four times the anti-SARS concentrations are designated "A" in parentheses (Fig. 3). The compounds of group B, however, showed 20% inhibition of cell growth at two times the anti-SARS concentrations.

Inhibition of Viral Replication Tested by ELISA, Western Blot Analysis, IFA, and Flow Cytometry Assay. Some of the anti-SARS compounds were evaluated at multiple concentrations to deduce the 50% inhibitory concentrations for the inhibition of viral replication (EC_{50}) and host growth (CC_{50}). The SI, the ratio of CC_{50} to EC_{50} (28), was used to evaluate these compounds. The most potent inhibitor found was compound **10** (Valinomycin), a peptide insecticide acting as a potassium ion transporter (29). The EC_{50} based on ELISA (Fig. 4) was 0.85 μM (SI = 80). The antiviral activity was further confirmed with IFA (Fig. 5) and Western blot and flow cytometry analysis (Fig. 6).

Compounds **5** (Aescin, a drug widely used in Europe) and **13**

BIOCHEMISTRY

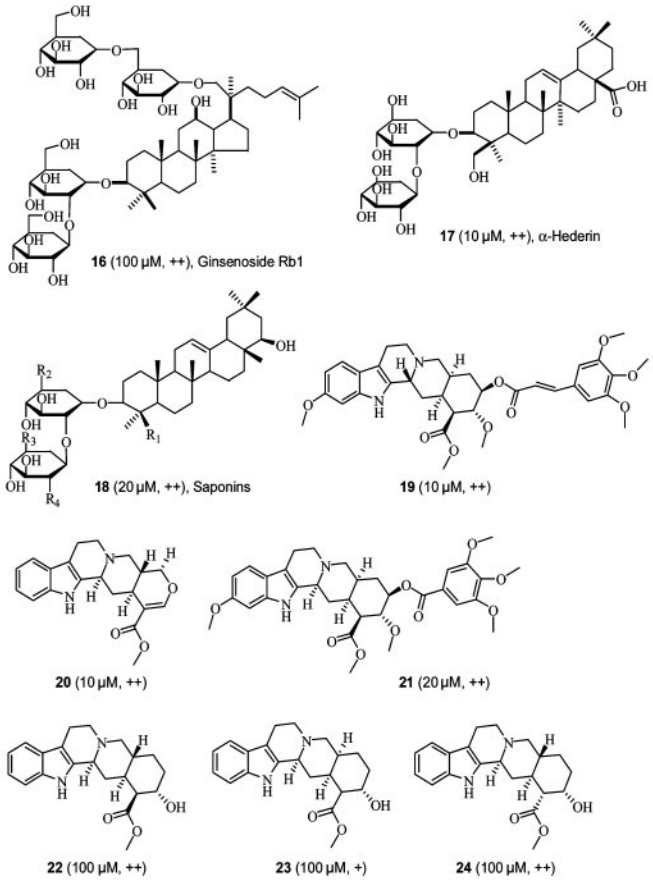

Fig. 7. The commercially available compounds whose structures have 80% similarity with Glycyrrihizin, Aescin, and Reserpine that showed anti-SARS-CoV activities <100 μM.

(Reserpine, a Food and Drug Administration-approved drug) were further tested with IFA, ELISA, Western blot analysis, and flow cytometry to confirm their anti-SARS activities. The EC_{50} values for Reserpine (compound **13**) and Aescin (compound **5**) were 3.4 μM and 6.0 μM, respectively, and the corresponding CC_{50} values were 25 μM (SI = 7.3) and 15 μM (SI = 2.5).

Aescin, the major active principle from the horse chestnut tree, has previously been used to treat patients with chronic venous insufficiency (30, 31), hemorrhoids (32), postoperative edema (30, 32), and inflammatory action (30, 33). Reserpine, a naturally occurring alkaloid produced by several members of the genus *Rauwolfia*, has been used primarily as a peripheral antihypertensive and as a central depressant and sedative (34). It has also found use as a radio-protective agent and experimentally as a contraceptive (35).

Because Glycyrrhizin, Aescin and Reserpine have been used clinically, their related natural products may be also active against SARS-CoV. We used the International Species Information System (ISIS) database to search for commercially available compounds whose structures have 80% similarities with these three drugs. We found 15 compounds related to Glycyrrhizin and Aescin and six compounds related to Reserpine. Through a cell-based assay, we found that 10 of the 21 compounds showed activities against SARS-CoV. Among them, four compounds (**6**, **16**, **17**, and **18**) are derivatives of Glycyrrhizin and Aescin, and all six derivatives of Reserpine (**19–24**) showed activities toward SARS-CoV at <100 μM. The structures and their minimal concentration of inhibition toward SARS-CoV are shown in Fig. 7. Ginsenoside-Rb1 (**16**) is one of

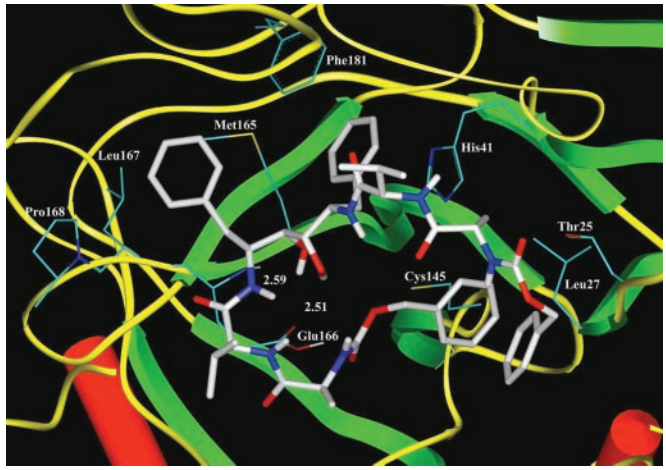

Fig. 8. Computer modeling of compound **2** binding to SARS-CoV 3CL protease. One of the two hydroxyl groups forms hydrogen bonds with Glu-166 through its side chain and the backbone amide bond. The phenyl groups fit into two pockets, one of which is well defined by hydrophobic residues (Met-165, Pro-168, and Leu-167).

the pharmacologically active components of the traditional Chinese herb, Panax ginseng (36). Glycyrrhizin has previously been reported to be active against SARS-CoV with $IC_{50} > 500$ μM (15).

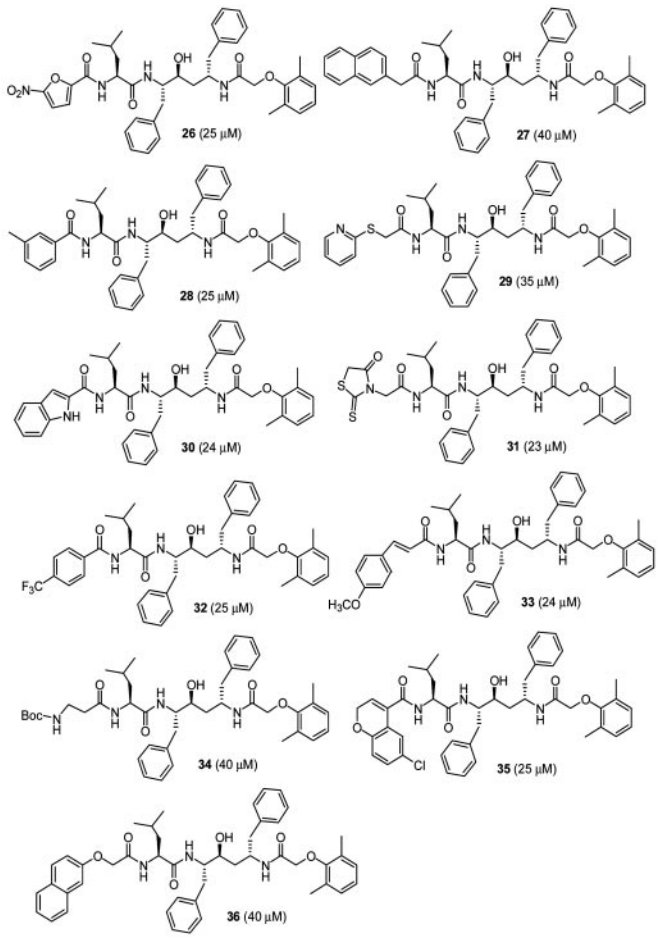

Fig. 9. The Lopinavir-like structures and their IC_{50} against 3CL protease.

Inhibition of SARS-3CL Protease. The main protease of SARS-CoV is a dimeric chymotrypsin-like protease called 3CL protease, with active-site Cys instead of Ser as nucleophile. Several synthetic inhibitors of the 3CL protease have been reported (22, 37), but are relatively weak and no further studies were conducted. Compounds **1** and **2** were developed as transition-state analog inhibitors of the HIV protease (38). The K_i value of **2** toward the HIV-protease is 1.5 nM and the feline immunodeficiency virus protease is 4 nM (ref. 39 and references therein). It is also active against several resistant variants in cell-based assays and effective in treatment of cats with AIDS (40). The K_i value of **2** against the SARS-CoV 3CL protease is 0.6 μM.

The docking simulation of compound **2** showed that the inhibitor is folded into a ring-like structure in the active site; one of the two hydroxyl groups forms hydrogen bonds with Glu-166 through its side chain and the backbone amide bond. The phenyl groups fit into two pockets, one of which is well defined by hydrophobic residues (Met-165, Pro-168, and Leu-167). The two Val side chains from the inhibitor seem to play no role in the affinity of **2**, because both of them point toward the solvent. However, whereas one of the Ala side chains is exposed to the solvent, the second one fits into a large pocket mostly defined by hydrophobic residues such as Leu-27 (Fig. 8). Further modification of **2** was carried out. Although removal of one of the two hydroxyl groups did not affect the protease inhibition activity, change of the Cbz group to the acetyl group or the Val residue to Gly or Ser reduced the activity significantly. Compound **2** was, however, bound in an extended form to the HIV and feline immunodeficiency virus proteases (ref. 39 and references therein); both are aspartyl proteases active as a C-2 symmetric dimer.

We have also tested the HIV protease inhibitors Ritonavir and Saquinavir, both used in the clinic, as inhibitors of SARS 3CL protease; however, neither showed activities at the concentration of 50 μM. Because Kaletra is a mixture of Lopinavir and Ritonavir, we tested Lopinavir alone, and its IC_{50} value was 50 μM (K_i = 14 μM). In an attempt to further improve its inhibition, we have also synthesized a series of derivatives of Lopinavir, but the best compound has an IC_{50} value of $\approx$25 μM (Fig. 9).

Other Anti-SARS CoV Compounds. Iminocyclitol **7** is an excellent inhibitor of α-fucosidase, with a K_i of $\approx$25 nM (41) toward human fucosidase; its inhibition against SARS-CoV is perhaps due to the disruption of the envelope glycoprotein processing. The two macrolides **11** and **12** perhaps target the viral RNA.

Some other well known traditional Chinese herbs were also tested in the cell-based assay and most of them were found inactive against SARS-CoV at the concentration of 10 μM. However, we found that extracts of eucalyptus and *Lonicera japonica* did show such activities at the concentration of 100 μM; and Ginsenoside-Rb1 (**17**), one of the pharmacologically active components of Panax ginseng (42, 43), also showed the antiviral activity at 100 μM. FP-21399, a bis-azo derivative with HIV inhibition activity by preventing viral entry (44), also exhibited inhibition activity at a low micromolar concentration, perhaps due to the same mechanism.

Finally, previous reports in the literature have predicted that several compounds may show antiviral activities against SARS, such as AG7088 (21), Pentoxifylline (45), Melatonin (46), and Vitamin C (47). However, our cell-based assay showed that these compounds had no effects at the concentration of 10 μM. Some other anti-RNA virus drugs, such as AZT, Didanosine, Nevirapine, Ritonavir, Lopinavir, Saquinavir, and Ribavirin, also showed no activities at the same concentration.

In summary, we have found 15 compounds with potent anti-SARS CoV activity, including two existing drugs. In addition, Valinomycin, FP-21399, and some saponins are highly effective and worth further study. HIV protease inhibitor **2** represents a promising candidate for further development because it has been shown active *in vivo* in cats with AIDS. Work should be done to determine the structure of the protease in complex with **2** for further optimization of the inhibitor.

We thank Drs. Lan Bo Chen and M. Ono at Harvard Medical School for FP-21399, Optimer (San Diego) for **11**–**12**, Microbio (Taipei, Taiwan) for *L. japonica*, Dr. Joseph C. Lin for Eucalyptus extract, Hui-Pei Tsai for help with flow cytometry, and Academia Sinica and National Science Council for their support.

1. Ksiazek, T. G., Erdman, D., Goldsmith, C. S., Zaki, S. R., Peret, T., Emery, S., Tong, S., Urbani, C., Comer, J. A., Lim, W., *et al.* (2003) *N. Engl. J. Med.* **348,** 1953–1966.
2. Peiris, J., Lai, S., Poon, L., Guan, Y., Yam, L., Lim, W., Nicholls, J., Yee, W. K., Yan, W. W., Cheung, M. T., *et al.* (2003) *Lancet* **361,** 1319–1311.
3. He, J.-F., Peng, G.-W., Min, J., Yu, D.-W., Liang, W.-J., Zhang, S.-Y., Xu, R.-H., Zheng, H.-Y., Wu, X.-W., Xu, J., *et al.* (2004) *Science* **303,** 1666–1669.
4. Peiris, J., Chu, C. M., Cheng, V. C. C., Chan, K. S., Hung, I. F. N., Poon, L. L. M., Law, K. I., Tang, B. S. F., Hon, T. Y. W., Chan, C. S., *et al.* (2003) *Lancet* **361,** 1767–1772.
5. So, L. K. Y., Lau, A. C. W., Yam, L. Y. C., Cheung, T. M. T., Poon, E., Yung, R. W. H. & Yuen, K. Y. (2003) *Lancet* **361,** 1615–1617.
6. Tsang, K. W., Ho, P. L., Ooi, G. C., Yee, W. K., Wang, T., Chan, Y. M., Lam, W. K., Seto, W. H., Yam, L. Y., Cheung, T. M., *et al.* (2003) *N. Engl. J. Med.* **348,** 1977–1985.
7. Poutanen, S. M., Low, D. E., Henry, B., Finkelstein, S., Rose, D., Green, K., Tellier, R., Draker, R., Adachi, D., Ayers, M., *et al.* (2003) *N. Engl. J. Med.* **348,** 1995–2005.
8. Lee, N., Hui, D., Wu, A., Chan, P., Cameron, P., Joynt, G. M., Ahuja, A., Yung, M. Y., Leung, C. B., To, K. F., *et al.* (2003) *N. Engl. J. Med.* **348,** 1986–1994.
9. Booth, C. M., Matukas, L. M., Tomlinson, G. A., Rachlis, A. R., Rose, D. B., Dwosh, H. A., Walmsley, S. L., Mazzulli, T., Avendano, M., Derkach, P., *et al.* (2003) *J. Am. Med. Assoc.* **289,** 2801–2809.
10. Chan, J. W., Ng, C. K., Chan, Y. H., Mok, T. Y., Lee, S., Chu, S. Y., Law, W. L., Lee, M. P. & Li, P. C. (2003) *Thorax* **58,** 686–689.
11. Tsui, P. T., Kwok, M. L., Yuen, H. & Lai, S. T. (2003) *Emerg. Infect. Dis.* **9,** 1064–1069.
12. Ho, J. C., Ooi, G. C., Mok, T. Y., Chan, J. W., Hung, I., Lam, B., Wong, P. C., Li, P. C., Ho, P. L., Lam, W. K., *et al.* (2003) *Am. J. Respir. Crit. Care Med.* **168,** 1449–1456.
13. Cinatl, J., Morgenstern, B., Bauer, G., Chandra, P., Rabenau, H. & Doerr, H. W. (2003) *Lancet* **361,** 2045–2046.
14. Tsang, K. & Seto, W. H. (2004) *Curr. Opin. Invest. Drugs* **5,** 179–185.
15. Cinatl, J., Morgenstern, B., Bauer, G., Chandra, P., Rabenau, H. & Doerr, H. W. (2003) *Lancet* **362,** 293–294.
16. Tan, E. L. C., Doi, E. E., Lin, C. Y., Tan, H. C., Ling, A. E., Lim, B. & Stanton, L. W. (2004) *Emerg. Infect. Dis.* **10,** 581–586.
17. Rota, P. A., Oberste, M. S., Monroe, S. S., Nix, W. A., Campagnoli, R., Icenogle, J. P., Penaranda, S., Bankamp, B., Maher, K., Chen, M.-h., *et al.* (2003) *Science* **300,** 1394–1399.
18. Marra, M. A., Jones, S. J. M., Astell, C. R., Holt, R. A., Brooks-Wilson, A., Butterfield, Y. S. N., Khattra J., Asano, J., K., Barber, S. A., Chan, S. Y., *et al.* (2003) *Science* **300,** 1399–1404.
19. Ruan, Y. J., Wei, C. L., Ee, A. L., Vega, V. B., Thoreau, H., Su, S. T., Chia, J. M., Ng, P., Chiu, K. P., Lim, L., *et al.* (2003) *Lancet* **361,** 1779–1785.
20. Li, W. H., Moore, M. J., Vasilieva, N., Sui, J., Wong, S. K., Berne, M. A., Somasundaran, M., Sullivan, J. L., Luzuriaga, K., Greenough, T. C., *et al.* (2003) *Nature* **426,** 450–454.
21. Annad, K., Ziebuhr, J., Wadhwani, P., Mesters, J. R. & Hilgenfeld, R. (2003) *Science* **300,** 1763–1767.
22. Yang, H., Yang, M., Ding, Y., Liu, Y., Lou, Z., Zhou, Z., Sun, L., Mo, L., Ye, S., Pang, H., *et al.* (2003) *Proc. Natl. Acad. Sci. USA* **100,** 13190–13195.
23. Fan, K., Wei, P., Feng, Q., Chen, S., Huang, C., Ma, L., Lai, B., Pei, J., Liu, Y., Chen, J., *et al.* (2004) *J. Biol. Chem.* **279,** 1637–1642.
24. Huang, C., Wei, P., Fan, K., Liu, Y. & Lai, L. (2004) *Biochemistry* **43,** 4568–4574.
25. Kuo, C.-J., Chi, Y.-H., Hsu, T.-A. & Liang, P.-H. (2004) *Biochem. Biophys. Res. Commun.* **318,** 862–867.
26. Morris, G. M., Goodsell, D. S., Halliday, R. S., Huey, R., Hart, W. E., Belew, R. K. & Olson, A. J. (1998) *J. Comput. Chem.* **19,** 1639–1662.
27. Buttke, T. M., McCubrey, J. A. & Owen, T. C. (1993) *J. Immunol. Methods* **157,** 233–240.
28. Khabar, K. S., al-Zoghaibi, F., Dzimiri, M., Taha, H., al-Tuwaijri, A. & al-Ahdal, M. N. (1996) *J. Interferon Cytokine Res.* **16,** 31–33.
29. Schneider, J. A. & Sperelakis, N. (1974) *Eur. J. Pharmacol.* **27,** 349–354.
30. Sirtori, C.-R. (2001) *Pharmacol. Res.* **44,** 183–193.
31. Frick, R.-W. (2000) *Angiology* **51,** 197–205.
32. Wilhelm, K. & Feldmeier, C. (1977) *Med. Klin.* **72,** 128–134.
33. Bazzoni, G., Dejana, E. & Del Maschio, A. (1991) *Haematologica* **76,** 491–499.
34. Fraser, H. S. (1996) *Clin. Pharmacol. Ther.* **60,** 368–373.
35. Chan, S. Y. W. & Tang, L. C. H. (1984) *Contraception* **30,** 363–369.
36. Jeong, C. S., Hyun, J. E. & Kim, Y. S. (2003) *Arch. Pharmacal Res.* **26,** 906–911.
37. Bacha, U., Barrila, J., Velazquez-Campoy, A., Leavitt, S. & Freire, E. (2004) *Biochemistry* **43,** 4906–4912.
38. Brik, A., Lin, Y.-C., Elder, J. H. & Wong, C.-H. (2002) *Chem. Biol.* **9,** 891–896.
39. Brik, A. & Wong, C.-H. (2003) *Org. Biomol. Chem.* **1,** 1–14.
40. Huitron-Resendiz. S., de Rozières, S., Sanchez-Alavez, M., Bühler, B., Lin, Y.-C., Lerner, D., Henriksen, N., Burudi, M., Fox, H., Torbett, B., *et al.* (2004) *Virology*, in press.
41. Wu, C.-Y., Chang, C.-F., Chen, J. S.-Y., Wong, C.-H. & Lin, C.-H. (2003) *Angew. Chem. Intl. Ed. Engl.* **42,** 4661–4664.
42. Tsai, S.-C., Chiao, Y.-C., Lu, C.-C. & Wang, P.-S. (2003) *Chin. J. Physiol.* **46,** 1–7.
43. Lee, Y.-J., Jin, Y.-R., Lim, W.-C., Park, W.-K., Cho, J.-Y., Jang, S. & Lee, S.-K. (2003) *Arch. Pharmacal Res.* **26,** 58–63.
44. Zhang, J., Hyeryn, C., Dezube, B., Farzan, M., Sharma, P., Zhou, X., Chen, L., Mitsunori, O., Gillies, S., Wu, Y., *et al.* (1998) *Virology* **244,** 530–541.
45. Martín, J. F. B., Jiménez, J. L. & Muñoz-Ferández, M. Á. (2003) *Med. Sci. Monit.* **9,** SR29–SR34.
46. Shiu, S. Y. W., Reiter, R. J., Tan, D.-X. & Pang, S. F. (2003) *J. Pineal Res.* **35,** 69–70.
47. Hemila, H. (2003) *J. Antimicrob. Chemother.* **52,** 1049–1050.

BIOCHEMISTRY